The Wavelength Dependence of the Photodissociation of Propionaldehyde in the 280−330 nm Region

Yunqing Chen and Lei Zhu*

Wadsworth Center, New York State Department of Health, Department of Environmental Health and Toxicology, State University of New York, Albany, New York 12201-0509

Received: April 18, 2001; In Final Form: June 26, 2001

We have investigated the photodecomposition of propionaldehyde (C_2H_5CHO; propanal) at 5 nm intervals in the 280−330 nm region by using dye laser photolysis combined with cavity ring-down spectroscopy. Absorption cross sections were determined for propionaldehyde. The HCO radical was a fragment from photodissociation. The HCO radical yields, obtained by monitoring its transient absorption at 613.8 nm, decreased with increasing C_2H_5CHO pressure in the 1−10 Torr range due to the increasing HCO + HCO, HCO + C_2H_5, and HCO + C_2H_5CHO reactions at higher propionaldehyde pressures and quenching by ground state propionaldehyde. After separating the contribution of HCO radical reactions, the propionaldehyde pressure quenching effect was only observed at photolysis wavelengths longer than 315 nm. Values of zero-pressure HCO yields (all λ) and ratios of quenching to unimolecular decay rate constant of excited propionaldehyde ($\lambda \geq 315$ nm) were given. The HCO yields (φ_{HCO}°) were 0.98 ± 0.06, 0.92 ± 0.06, 0.95 ± 0.08, 0.98 ± 0.11, 0.91 ± 0.05, and 1.08 ± 0.07 at 295, 300, 305, 310, 315, and 320 nm, indicating that $C_2H_5CHO + h\nu \rightarrow C_2H_5 + HCO$ is the dominant photolysis pathway. The HCO yields decreased at both the shorter-wavelength (280 nm) and the longer-wavelength (330 nm) ends. The wavelength dependence of the HCO yields from propionaldehyde photolysis was compared to that from *t*-pentanal ($(CH_3)_3CCHO$) photolysis. The HCO yields from *t*-pentanal photolysis decayed much more rapidly at the shorter-wavelength end, which might reveal the difference in the excited states singlet−triplet surface crossing of *t*-pentanal versus propionaldehyde. The dependence of the HCO yields on nitrogen buffer gas pressure was examined between 10 and 400 Torr. No dependence was observed. Cross section results were combined with HCO radical yields to estimate atmospheric photodissociation rate constants of propionaldehyde to form HCO as a function of zenith angle for cloudless conditions and at 760 Torr nitrogen pressure. Radical formation rate constants were $1.6 \times 10^{-5} - 4.6 \times 10^{-5}$ s^{-1} for zenith angles of 0−60°.

Introduction

Aliphatic aldehydes are key constituents of the photochemical smog cycles. Their photodissociation is an important source of free radicals in the atmosphere. Aldehydes are introduced into the ambient environment through biogenic and anthropogenic emissions or through photo-oxidation of tropospheric organic compounds. The major degradation pathways for saturated aliphatic aldehydes in the atmosphere are reactions with OH radicals and unimolecular photodissociation. Rate constants for OH radical reactions with C_1-C_5 aldehydes have been reported previously.[1−4] The photolysis of formaldehyde (CH_2O) and acetaldehyde (CH_3CHO) has been studied extensively.[5−8] Previous studies on the photodecomposition of propionaldehyde (C_2H_5CHO, propanal) have been carried out at a few irradiation wavelengths in the actinic UV region,[9−11] and the peak radical yield reported by the same group[9,10] differed by almost a factor of 4. Recently, Terentis and co-workers[12,13] reported the nascent state distribution of the HCO photoproduct from the 308 and 309 nm photolysis of propionaldehyde, but they did not obtain the HCO radical yields. Determination of the wavelength-dependent photolysis quantum yields of propionaldehyde allows a comparison with those reported previously for formaldehyde and acetaldehyde[5−8] and with our recent results on C_5 aldehydes.[14,15] It also permits an estimation of atmospheric radical formation rate constants from propionaldehyde photolysis.

Propionaldehyde exhibits a broad absorption band in the 240−360 nm region as a result of an electric dipole-forbidden but vibronically allowed n → π^* transition.[16] A number of primary decomposition processes are thermodynamically allowed following excitation of propionaldehyde in the near-UV region:

$$C_2H_5CHO + h\nu \rightarrow C_2H_6 + CO \qquad (\text{all } \lambda) \qquad (1)$$

$$\rightarrow C_2H_5 + HCO \qquad \lambda \leq 341 \text{ nm} \qquad (2)$$

$$\rightarrow C_2H_4 + H_2CO \qquad \lambda \leq 0.91\ \mu\text{m} \qquad (3)$$

$$\rightarrow CH_3 + CH_2CHO \qquad \lambda \leq 345 \text{ nm} \qquad (4)$$

where the photochemical thresholds were calculated from the corresponding enthalpy changes. Previous end-product study indicated that reactions 3 and 4 were very minor ($\varphi_3 \approx 0.003$ and $\varphi_4 \approx 0.00$ at 313 nm) in the actinic UV region.[11]

In this paper, we present results obtained from an investigation of the photolysis of propionaldehyde at 5 nm intervals in the 280−330 nm region by combining dye laser excitation with cavity ring-down spectroscopy.[17,18] Absorption cross sections of propionaldehyde were determined at each wavelength studied. The formation yields of HCO and their dependence on photodissociation wavelength, propionaldehyde pressure, and total

* To whom correspondence should be addressed: zhul@orkney.ph.albany.edu (e-mail); (518) 473-2895 (fax).

10.1021/jp011445s CCC: $20.00
Published on Web 10/03/2001

pressure were obtained. Absolute HCO radical concentration was calibrated relative to those obtained from formaldehyde photolysis or from the $Cl + H_2CO \rightarrow HCl + HCO$ reaction. The cross section result was combined with HCO yield information to estimate photodissociation rate constants and lifetimes of C_2H_5CHO as a function of zenith angle for cloudless conditions at sea level and at 760 Torr nitrogen pressure.

Experimental Section

The experimental apparatus has been described in detail elsewhere.[14,15,19,20] The photolysis laser system consisted of the frequency-doubled output of a tunable dye laser pumped by a 308 nm XeCl excimer laser (~200 mJ/pulse). Laser dyes used included Coumarin 153, Rhodamine 6G, Rhodamine B, Rhodamine 101, Sulfurhodamine 101, and DCM. The excitation laser pulse propagated into a stainless steel reaction cell at a 15° angle with the main cell axis through a sidearm, while the probe laser pulse (613−617 nm) from a nitrogen-pumped dye laser was introduced along its main optical axis. The pump and the probe laser beams were overlapped in the middle of the reaction cell vacuum-sealed with a pair of high-reflectance cavity mirrors. The base path length between the two cavity mirrors was 50 cm. A fraction of the probe laser output was transmitted into the cavity through the front mirror. The laser light that was trapped in the cavity bounced back and forth many times and decayed by loss mechanisms such as mirror loss and sample absorption. The photon intensity decay inside the cavity was detected by measuring the light exiting the rear mirror with a photomultiplier tube (PMT). The PMT output was amplified, digitized, and passed to a computer. The decay curve was fitted to a single-exponential decay function. The ring-down time constant and the total loss per optical pass were calculated. The ring-down time constant was on the order of 27 μs for an empty cavity with 60 ppm transmission loss per mirror. In the presence of absorbing species, the cavity decay time shortened. By measurement of cavity losses with and without a photolysis pulse, HCO absorption from the photolysis of propionaldehyde was obtained. The photolysis laser pulse energy was monitored with a calibrated Joulemeter.

Gas pressure was measured in the middle of the reaction cell with a capacitance manometer. Quantum yields were acquired at a laser repetition rate of 0.1 Hz to ensure replenishment of the gas sample between successive laser pulses. Spectrum scan was carried out at a laser repetition rate of 1 Hz. All experiments were conducted at an ambient temperature of 293 ± 2 K.

Propionaldehyde (≥97% purity; Aldrich) was degassed by several freeze−pump−thaw cycles and was pumped at liquid nitrogen temperature for at least 30 min before each experimental run to remove volatile impurities. Formaldehyde was produced from pyrolysis of polymer paraformaldehyde (≥95% purity; Aldrich) at 110 °C. Nitrogen (≥99.999% purity; Praxair) and chlorine (≥99.5% purity; Matheson) were used without further purification.

Results and Discussion

Absorption Cross Sections of Propionaldehyde in the 280−330 nm Region. The room-temperature absorption cross sections of propionaldehyde were acquired at 5 nm intervals for the wavelength region from 280 to 330 nm. They are shown in Figure 1 and summarized in Table 1. The absorption cross section at each wavelength was obtained by monitoring the transmitted photolysis photon intensity as a function of propionaldehyde pressure in the cell and by applying Beer's law to the data obtained. Error bars quoted (1σ) are the estimated

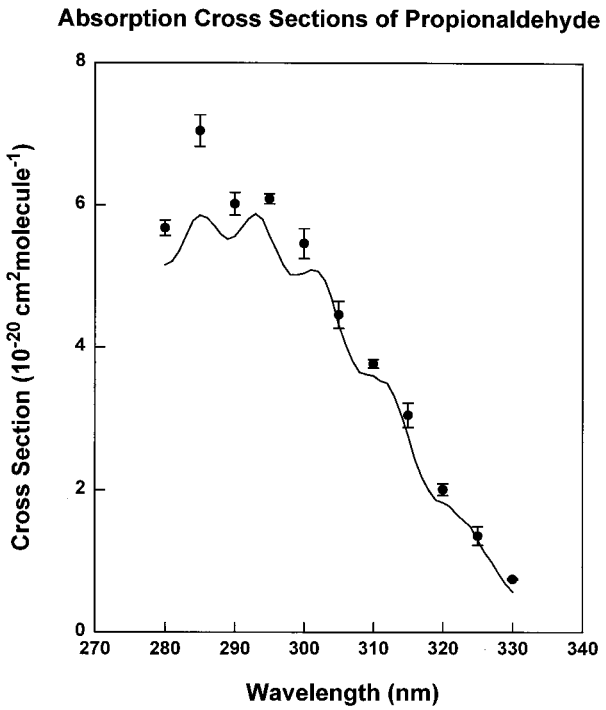

Figure 1. Absorption cross sections of propionaldehyde in the 280−330 nm region. Solid line, cross sections reported by Martinez and co-workers;[16] circles, those determined in this work.

TABLE 1: Absorption Cross Sections of Propionaldehyde

λ (nm)	σ (10^{-20} cm^2 molecule^{-1})
280	5.68 ± 0.11
285	7.05 ± 0.22
290	6.02 ± 0.16
295	6.09 ± 0.07
300	5.46 ± 0.21
305	4.46 ± 0.19
310	3.77 ± 0.06
315	3.05 ± 0.17
320	2.01 ± 0.08
325	1.36 ± 0.13
330	0.75 ± 0.01

precision of cross section determination, which includes the standard deviation for each measurement (~0.5%) plus the standard deviation about the mean of at least four repeated experimental runs. In addition to random errors, systematic errors such as uncertainty in the determination of pressure (0.1%) and path length (0.2%) and the presence of impurity (<3% impurity; mostly water) in propionaldehyde also contribute to the uncertainty in cross section values. The overall uncertainty for cross section measurements considering both random (see Table 1) and systematic errors is about 5−10% for all wavelengths studied. Included in Figure 1 for comparison are cross section results reported by Martinez and co-workers.[16] Except for 285 and 330 nm, our cross section data agree to within 10% with those obtained by that group.[16] Our cross section values at 285 and 330 nm are 20% and 30% larger than those obtained previously while the reason for this difference is unclear.

Time-Resolved Studies of the Photolysis of Propionaldehyde in the 280−330 nm Region. A portion of the cavity ring-down absorption spectrum of the product after 290 nm photolysis of propionaldehyde is displayed in Figure 2. Also shown in the same figure is a previously reported absorption spectrum[21] of HCO in the same wavelength region. The similarity of these two spectra indicates that the HCO radical

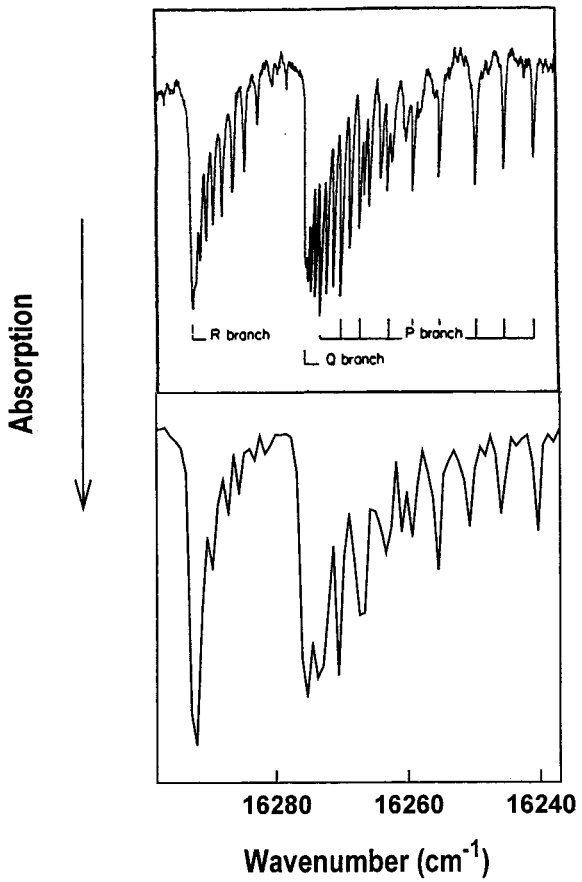

Figure 2. Lower trace: low-resolution cavity ring-down absorption spectrum of the product after 290 nm photolysis of 5.05 Torr C_2H_5-CHO. Upper trace: intracavity laser absorption spectrum of the (000) → (090) vibronic transition of HCO following photolysis of 0.1 Torr CH_3CHO/10 Torr Ar at 266 nm (adapted from ref 21).

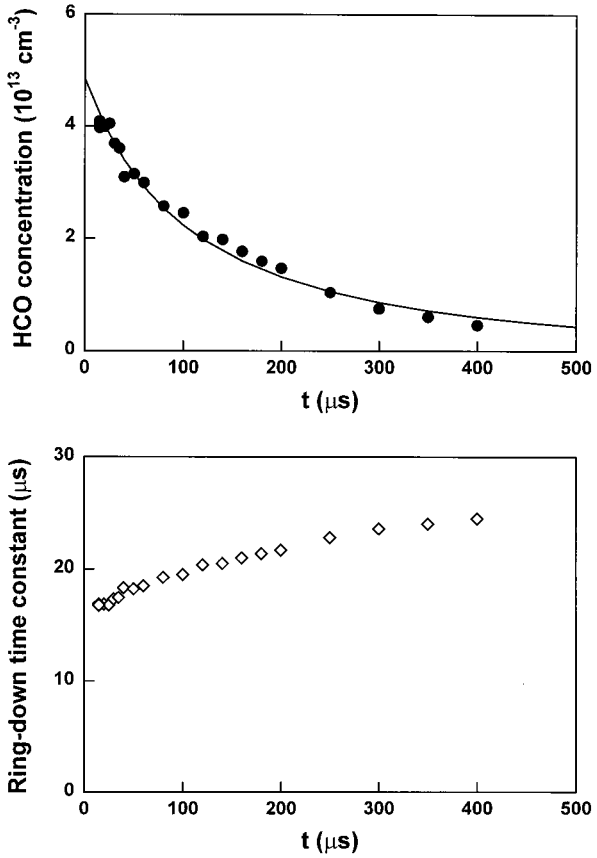

Figure 3. Upper figure: time profile of the HCO radical from the photolysis of 3 Torr propionaldehyde at 290 nm. Circles, experimental results; solid line, simulated profile calculated using the ACUCHEM simulation program. Bottom figure: experimental ring-down time constant as a function of time.

is a photodissociation product of propionaldehyde. The cavity ring-down spectrometer was tuned to the HCO $X^2A''(0,0,0) \rightarrow A^2A'(0,9,0)$ R bandhead at 613.8 nm, and the HCO concentration was followed as a function of time. Shown in Figure 3 is a temporal profile of HCO from 290 nm photolysis of 3 Torr propionaldehyde along with a fit consisting of the following kinetic scheme:

$$HCO + HCO \rightarrow H_2CO + CO \quad (5)$$

$$HCO + C_2H_5 \rightarrow \text{products} \quad (6)$$

$$C_2H_5 + C_2H_5 \rightarrow C_4H_{10} \quad (7a)$$

$$\rightarrow C_2H_4 + C_2H_6 \quad (7b)$$

$$HCO + C_2H_5CHO \rightarrow \text{products} \quad (8)$$

Also displayed in Figure 3 is a plot of the experimental ring-down time constant as a function of time. As seen from Figure 3, HCO concentration decays to its 1/e value in about 190 μs, while the ring-down time constant varies from ~17 μs to ~21 μs in this interval. The kinetic scheme that was used to model HCO decay assumes that the HCO + C_2H_5 channel is the only important radical formation channel from the photolysis of propionaldehyde at 290 nm, an assumption which is supported by the approximately unity HCO quantum yield ($\varphi = 0.95 \pm 0.06$) described later in this paper. Time-resolved HCO decay profiles from the photodissociation of propionaldehyde at 3, 6, and 9 Torr pressure were compared with those calculated by the ACUCHEM simulation program.[22] The following input parameters were used: rate constants for HCO + HCO, HCO + C_2H_5, C_2H_5 + C_2H_5, and HCO + C_2H_5CHO reactions ($k_{HCO+HCO}$, $k_{HCO+C2H5}$, $k_{C2H5+C2H5}$, and $k_{HCO+C2H5CHO}$) and the initial HCO concentration ($[HCO]_0$). The literature value of $k_{C2H5+C2H5}$ (1.9×10^{-11} cm^3 molecule^{-1} s^{-1}) was used in the fitting.[23] Initial values of $k_{HCO+HCO}$, $k_{HCO+C2H5}$, and $k_{HCO+C2H5CHO}$ were given to the program, and the fitted HCO profiles were compared with the experimental results. After several iterations and adjustment of $k_{HCO+HCO}$, $k_{HCO+C2H5}$, and $k_{HCO+C2H5CHO}$ values, best fits of the experimental profiles were accomplished. $k_{HCO+HCO}$, $k_{HCO+C2H5}$, and $k_{HCO+C2H5CHO}$ thus extracted were $(6.0 \pm 1.5) \times 10^{-11}$, $(6.5 \pm 1.5) \times 10^{-11}$, and $(1.5 \pm 0.2) \times 10^{-14}$ cm^3 molecule^{-1} s^{-1}, respectively, where uncertainty (1σ) represents experimental scatter only. The HCO decay profiles at all three aldehyde pressures were well fitted by the extracted $k_{HCO+HCO}$, $k_{HCO+C2H5}$, and $k_{HCO+C2H5CHO}$ values. Accuracy in $k_{HCO+HCO}$ and $k_{HCO+C2H5}$ was affected by accuracy of $[HCO]_0$ and the time resolution of the cavity ring-down spectroscopy (~17−21 μs around 613 nm). The initial HCO concentration was in the range of 4.8×10^{13} to 8.5×10^{13} cm^{-3} for propionaldehyde pressures between 3 and 9 Torr. The overall uncertainty that includes both random and systematic errors in the extracted values of $k_{HCO+HCO}$ and $k_{HCO+C2H5}$ was about 50%. Values of $k_{HCO+HCO}$ and $k_{HCO+C2H5}$ thus obtained agree well with the recommended rate constant[24] for the HCO + HCO reaction ($k = 2.5 \times 10^{-11}$−10.0×10^{-11} cm^3 molecule^{-1} s^{-1} at 300 K) and the previously reported rate constant[25] for C_2H_5 + HCO reaction ($(7.2 \pm 1.6) \times 10^{-11}$ cm^3 molecule^{-1} s^{-1}).

TABLE 2: Absorption Cross Sections of Formaldehyde and Chlorine

λ (nm)	σ_{H2CO} (10^{-20} cm^2)	σ_{Cl2} (10^{-20} cm^2)
280	2.04 ± 0.17	
285	3.52 ± 0.18	
290	1.08 ± 0.26	
295	3.76 ± 0.71	
300	0.81 ± 0.13	
305	4.20 ± 0.44	
310	1.27 ± 0.12	18.4 ± 0.2
315		21.3 ± 0.7
320		23.4 ± 1.0
325		24.5 ± 0.8
330		24.8 ± 0.9

The value of $k_{HCO+C2H5CHO}$ influences mostly the HCO decay profile at time scale on the order of hundreds of microseconds. Since the HCO decay profiles were measured at several propionaldehyde pressures and under conditions $[HCO]_0 \ll [C_2H_5CHO]_0$, the overall uncertainty in the $k_{HCO+C2H5CHO}$ value was about ~20%.

HCO Radical Yields from the Photolysis of Propionaldehyde in the 280−330 nm Region. The HCO radical yield from the photolysis of propionaldehyde was determined from the ratio of the HCO concentration produced in the photolysis/probe laser overlapping region to the absorbed photon density in the same region. The overlapping region could be viewed as a rectangular solid with width and height defined by those of the photolysis beam, and length defined by (beam width) × tan(15°)$^{-1}$, where 15° is the angle (≤±0.5° uncertainty in angle measurement) between the photolysis and the probe beams. The widths of the photolysis beam varied between 1.1 and 1.8 mm, depending on the identity of the laser dyes used while the uncertainty in the beam width measurement was ~15%. Thus, the length of the photolysis/probe laser overlapping region was between 4.1 ± 0.6 and 6.7 ± 1.0 mm. Because the photolysis beam was absorbed by propionaldehyde over the entire level arm through which it traveled, the absorption of the photolysis beam by propionaldehyde in the pump/probe laser overlapping region could be derived from the difference in the transmitted photolysis photon intensities at the beginning and at the end of the overlapping region. The photolysis photon fluence was measured by a calibrated Joulemeter. The absorbed photon density in the photolysis/probe laser overlapping region at a given initial propionaldehyde pressure could be calculated once we knew the incident photon fluence into the cell and the absorption cross section of propionaldehyde at the photodissociation wavelength. The HCO concentration generated from the photolysis was acquired by measuring its absorption at 613.80 nm at a photolysis and a probe laser delay of 15 μs. To convert HCO absorption into absolute concentration, the absorption cross section of HCO at the probe laser wavelength was determined relative to the photolysis reaction $H_2CO + h\nu \rightarrow HCO + H$, for which the HCO quantum yield is known,[24] or from the Cl + $H_2CO \rightarrow$ HCl + HCO reaction. Formaldehyde photolysis calibration was used in the 280−310 nm region. H_2CO was produced immediately before each calibration run in a glass bulb. The purity of H_2CO was estimated by comparing its absorption cross section values with literature values.[26] The H_2CO absorption cross section was determined by measuring the transmitted photolysis photon fluence as a function of H_2CO pressure in the cell, and by applying Beer's law to the data obtained. Our H_2CO cross section data (listed in Table 2) agreed to within 10% with those obtained by Meller and Moortgat[26] at 290 and 295 nm, to within 15% at 280, 285, and 305 nm, to within 20% at 300 nm, and to within 30% at 310 nm. Since the HCO absorption was measured at 15 μs after the photolysis of H_2CO, the following sequence of reactions have been used to calculate HCO concentration at $t = 15$ μs (HCO concentration at $t = 0$ was calculated from the absorbed photon density at the photolysis/probe laser overlapping region and the literature[24] HCO yields from H_2CO photolysis):

$$HCO + HCO \rightarrow H_2CO + CO \quad (5)$$

$$H + HCO \rightarrow H_2 + CO \quad (9)$$

$$H + H_2CO \rightarrow H_2 + HCO \quad (10)$$

A $k_{HCO+HCO}$ value of 6.0×10^{-11} cm^3 molecule^{-1} s^{-1} determined from this work was used in the fitting. Literature k_{H+HCO} and k_{H+H2CO} values of 1.5×10^{-10} and 3.8×10^{-14} cm^3 molecule^{-1} s^{-1} were also used in the simulation.[23] In the 310−330 nm region, the Cl + H_2CO reaction was used to calibrate the absolute HCO concentration. The Cl + H_2CO calibration was conducted by first introducing only H_2CO into the cell and determined the HCO radical absorption resulting from the formaldehyde photolysis. A mixture of chlorine (Cl_2) and H_2CO was subsequently introduced into the cell, and the sum of HCO absorption from the Cl + H_2CO reaction and the photolysis of H_2CO was measured. The difference in the HCO absorption with and without Cl_2 but with equal amount of H_2CO gave the HCO absorption resulting from the Cl + H_2CO reaction (the ratio of HCO absorption due to the photolysis of H_2CO to the total absorption was approximately 28%, 32%, 16%, 8%, and 10% at 310, 315, 320, 325, and 330 nm). Chlorine (Cl_2) and formaldehyde were introduced into the cell at a pressure ratio $P_{Cl2}/P_{H2CO} = 1{:}5$ ($P_{total} = 0.6$ and 1.2 Torr) in order to ensure that Cl atoms produced from the photolysis of Cl_2 reacted only with H_2CO. Absorption cross sections of Cl_2 were determined in the 310−330 nm region and are tabulated in Table 2; they agreed with literature values[27] to within 5% at all wavelengths. The following sequence of reactions can occur at 15 μs after the photolysis of a Cl_2/H_2CO mixture:

$$Cl + H_2CO \rightarrow HCl + HCO \quad (11)$$

$$HCO + Cl_2 \rightarrow HClCO + Cl \quad (12)$$

$$Cl + H_2CO \rightarrow HCl + HCO \quad (13)$$

To account for the regeneration of HCO through reactions 12 and 13, literature $k_{HCO+Cl2}$ and $k_{Cl+H2CO}$ values of 7.6×10^{-12} and 7.3×10^{-11} cm^3 molecule^{-1} s^{-1} were used in the simulation.[24,28] Regeneration of HCO through reactions 12 and 13 increased HCO yields by 1% under the experimental condition used and has been accounted for. At 310 nm, both formaldehyde photolysis and the Cl + H_2CO reaction were used to calibrate absolute HCO concentration. The HCO absorption cross section obtained by these two methods agreed to within 9%.

The dependence of the HCO radical yields on propionaldehyde pressure was examined by measuring the HCO radical yields from the photolysis of 1, 2, 4, 6, 8, and 10 Torr of propionaldehyde. Displayed in Figure 4 are plots of the HCO yields (φ_{HCO}) as a function of propionaldehyde pressure resulting from photodissociation at 290 and 320 nm. φ_{HCO} decreased with increasing propionaldehyde pressure, possibly due to the quenching of the excited precursor to dissociation by the ground-state propionaldehyde molecules and the increasing HCO + HCO, C_2H_5 + HCO, and HCO + C_2H_5CHO reactions at higher propionaldehyde pressures. To separate the contribution of HCO radical reactions from the quenching process, both the

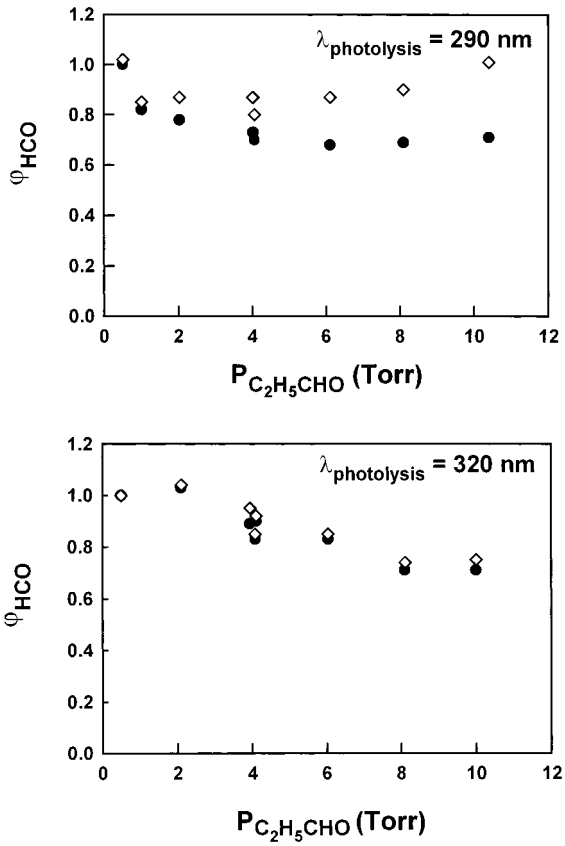

Figure 4. HCO radical yields as a function of C_2H_5CHO pressure from 290 and 320 nm photolysis. Circles: uncorrected yields. Diamonds: yields that have been corrected for HCO + HCO, HCO + C_2H_5, and HCO + C_2H_5CHO reactions at 15 μs.

uncorrected HCO yields and the yields that have been corrected for HCO radical reactions at 15 μs were included in Figure 4. As seen from Figure 4, there was no propionaldehyde pressure quenching effect when photolysis study was conducted at 290 nm. The corrected HCO radical yields still decreased with increasing propionaldehyde pressure at 320 nm, suggesting a quenching effect at longer photolysis wavelengths. Since 320 nm is close to the photodissociation threshold of propionaldehyde, increasing propionaldehyde pressure quenched the excited molecule to below its dissociation limit. The corrected reciprocal HCO yields were plotted against propionaldehyde concentration ([C_2H_5CHO]) according to the Stern−Volmer equation:

$$1/\varphi_{HCO} = 1/\varphi_{HCO}^{\circ} + (k^{Q}_{C2H5CHO}/k^{D}_{C2H5CHO})\cdot[C_2H_5CHO] \quad (14)$$

where φ_{HCO}° is the HCO yield extrapolated to zero propionaldehyde pressure and $k^{Q}_{C2H5CHO}/k^{D}_{C2H5CHO}$ is the ratio of quenching to unimolecular decay rate constant of excited propionaldehyde. For those photolysis wavelengths where the corrected HCO yields were independent of propionaldehyde pressure, $k^{Q}_{C2H5CHO}/k^{D}_{C2H5CHO}$ is equal to zero. Illustrated in Figure 5 is a plot of $1/\varphi_{HCO}$ versus [C_2H_5CHO] at 320 nm photodissociation wavelength; note that it is linear. Values of φ_{HCO}° (all λ) and $k^{Q}_{C2H5CHO}/k^{D}_{C2H5CHO}$ ($\lambda \geq 315$ nm) as a function of the photolysis wavelength are tabulated in Table 3 and plotted in Figure 6 (φ_{HCO}° only). Coefficients of $k^{Q}_{C2H5CHO}/k^{D}_{C2H5CHO}$ are $(9.4 \pm 5.2) \times 10^{-19}$, $(1.4 \pm 0.4) \times 10^{-18}$, $(1.9 \pm 0.6) \times 10^{-18}$, and $(1.7 \pm 0.9) \times 10^{-18}$ cm^3/molecule at 315, 320, 325, and 330 nm. $k_{C2H5CHO}{}^{D}$ has been reported to be around 2.4×10^8 s^{-1} for an excited propionaldehyde (S_1 state, $E_{vib} \approx 0$), which

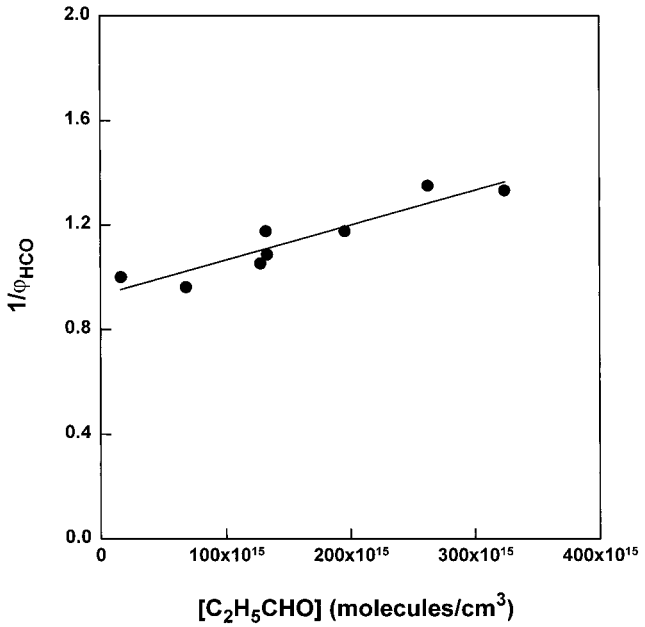

Figure 5. Stern−Volmer plot of the reciprocal HCO yields from 320 nm photolysis of C_2H_5CHO. Circles, experimental data; solid line, fit to the Stern−Volmer expression.

TABLE 3: Values of φ^{0}_{HCO} and $k^{Q}_{C2H5CHO}/k^{D}_{C2H5CHO}$ vs Wavelengths from Propionaldehyde Photolysis

λ (nm)	φ^{0}_{HCO}	$k^{Q}_{C2H5CHO}/k^{D}_{C2H5CHO}$ (cm^3/molecule)
280	0.85 ± 0.06	0
285	1.01 ± 0.07	0
290	0.95 ± 0.06	0
295	0.98 ± 0.06	0
300	0.92 ± 0.06	0
305	0.95 ± 0.08	0
310	0.98 ± 0.11	0
315	0.91 ± 0.05	$(9.4 \pm 5.2) \times 10^{-19}$
320	1.08 ± 0.07	$(1.4 \pm 0.4) \times 10^{-18}$
325	1.07 ± 0.14	$(1.9 \pm 0.6) \times 10^{-18}$
330	0.84 ± 0.08	$(1.7 \pm 0.9) \times 10^{-18}$

translates into an excited-state decay lifetime of ~4 ns.[29] Therefore, $k^{Q}_{C2H5CHO}$ is on the order of $2.3\times-4.6 \times 10^{-10}$ cm^3 molecule^{-1} s^{-1}. The magnitude of $k^{Q}_{C2H5CHO}$ is reasonable since an electronic-to-vibrational energy transfer (E → V) can occur on a single collision time scale. Values of φ_{HCO}° were approximately unity in the 285−325 nm region and then decreased at both the longer and the shorter-wavelength ends. The HCO yields decreased with decreasing wavelengths at $\lambda < 285$ nm, possibly due to the opening up of an additional photodissociation pathway such as a molecular elimination channel at higher photon energies. The reduced HCO yield at the longer-wavelength tail (330 nm) is probably the result of photodissociation at near-threshold wavelength. The error bars were calculated using cumulated error analysis of the standard deviations of at least two $1/\varphi_{HCO}$ versus [C_2H_5CHO] plots. Systematic errors include uncertainties in the determination of the following parameters: HCO concentration and absorption cross section (~20% at propionaldehyde pressures up to 4 Torr; HCO concentration correction is large at higher propionaldehyde pressure, but the zero pressure yield is close to the low-pressure yield data), propionaldehyde concentration (~3%) and absorption cross section (~5%), pulse energy (5%), angle between photolysis and probe laser (3%), and the dye laser width. Since the HCO radical yields from the photolysis of propionaldehyde

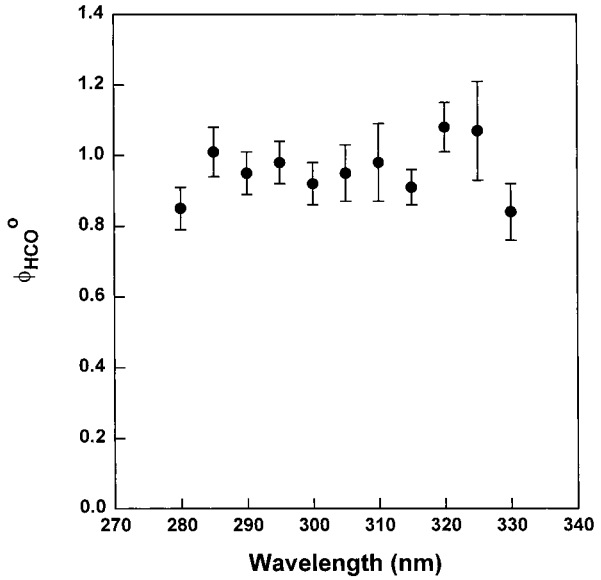

Figure 6. HCO radical yields extrapolated to zero propionaldehyde pressure as a function of photodissociation wavelength.

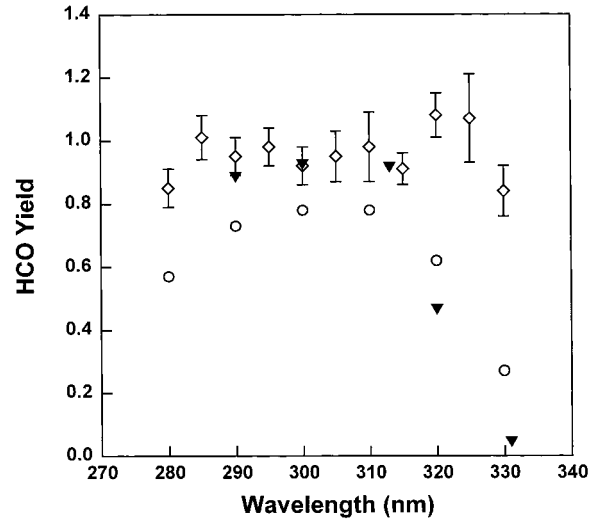

Figure 7. Wavelength dependency of radical yields from the photolysis of formaldehyde, acetaldehyde, and propionaldehyde. Circles, formaldehyde from ref 5; inverted triangles, acetaldehyde from ref 8; diamonds, propionaldehyde from this work.

were determined relative to those obtained from H_2CO photolysis or from the $Cl + H_2CO$ reaction, uncertainty in dye laser width measurement should not directly affect the relative photodissociation yield but it will affect correction of HCO radical reactions. As a result, uncertainty in dye laser width will indirectly affect the yield data. The overall uncertainty in the determination of φ_{HCO}° was about 40−50% in the wavelength range studied.

The dependence of the HCO radical yields on total pressure was examined by maintaining a constant propionaldehyde pressure and varying the nitrogen carrier gas pressure. The HCO radical yields were found to be independent of total pressure to within the experimental error limit when the total pressure was varied between 8 and 400 Torr in the 280−330 nm region. In the presence of excess nitrogen, there could be an electronic-to-rotational/translational energy transfer (E → R/T) and a vibrational-to-rotational/translational energy transfer (V → R/T) between the vibronically excited propionaldehyde and nitrogen, but these processes are not efficient. While in the case of photolysis of several Torr of propionaldehyde, an electronic-to-vibrational energy transfer (E → V) and a resonant vibrational-to-vibrational energy transfer (V → V) between the excited and the ground-state propionaldehyde may occur, and such processes can be very efficient. Therefore, observation of pressure quenching by propionaldehyde at several Torr pressures at longer photolysis wavelengths does not necessary indicate a discrepancy with the absence of quenching by nitrogen at pressures of 400 Torr. The HCO radical yields listed in Table 3 are set equal to those obtained from the photolysis of propionaldehyde at 760 Torr nitrogen pressure.

Shepson and Heicklen[9] measured CO and C_2H_6 quantum yields from photodissociation of propionaldehyde in air. Quantum yields for the $C_2H_5 + HCO$ channel were obtained from the difference in the quantum yields of CO and C_2H_6; they were 0.13, 0.28, 0.22, 0.26, 0.067, and 0.18 at 254, 280, 302, 313, 326, and 334 nm at 760 Torr air pressure. Heicklen and co-workers[10] acquired C_2H_5 quantum yields by either flash photolysis of propionaldehyde in air and monitoring of the UV absorption of total peroxy radicals ($C_2H_5O_2 + HO_2$) at 250 nm or by steady-state photolysis of propionaldehyde in oxygen. Their C_2H_5 yields were 0.89, 0.85, 0.50, 0.26, and 0.15 at 294, 302, 313, 325, and 334 nm in air at 760 Torr. Our HCO yields from propionaldehyde photolysis are 0.85 ± 0.06, 1.01 ± 0.07, 0.95 ± 0.06, 0.98 ± 0.06, 0.92 ± 0.06, 0.95 ± 0.08, 0.98 ± 0.11, 0.91 ± 0.05, 1.08 ± 0.07, 1.07 ± 0.14, and 0.84 ± 0.08 at 280, 285, 290, 295, 300, 305, 310, 315, 320, 325, and 330 nm at 760 Torr nitrogen pressure. Our HCO yields are much larger than the C_2H_5 yields reported by Shepson and Heicklen.[9] There is a good agreement between the 295 and 300 nm HCO yields determined in this work and the 294 and 302 nm C_2H_5 yields reported by Heicklen and co-workers.[10] However, our 315 and 325 nm HCO yields are 1.8−4.1 times the previously reported 313 and 325 nm C_2H_5 yields. Since both the ground state of oxygen and the first electronically excited state of propionaldehyde are triplet, there might be an electronic-to-electronic energy transfer (E → E) between excited propionaldehyde and oxygen. This quenching effect would become more apparent at the longer-wavelength tail where dissociation is near threshold. Another plausible explanation for this difference in radical yields with and without oxygen is that the absorption cross sections of propionaldehyde are small at the longer photodissociation wavelengths. This fact, plus the complex chemistry involved in the presence of oxygen, might subject the previous results to more uncertainties.

Comparison with the Photolysis of Other Aldehydes. Our results on the propionaldehyde photolysis were compared with those reported previously on formaldehyde[5] and acetaldehyde[8] to highlight their similarities and differences. Radical products were formed from photodissociation of all three aldehydes. Radical yields as a function of wavelength from the photolysis of formaldehyde,[5] acetaldehyde,[8] and propionaldehyde are shown in Figure 7. The radical yields decrease at both the longer and the shorter-wavelength ends. The peak radical yields are ∼0.8, ∼0.9 (at low pressure), and ∼1.0 from the photolysis of formaldehyde, acetaldehyde, and propionaldehyde, respectively. The photodecomposition mechanism somewhat differs for these three aldehydes. For formaldehyde photolysis, internal conversion (IC) of the excited S_1 state to the ground S_0 state dominates over intersystem crossing (ISC) to the first excited triplet state (T_1) over a wide range of excitation energies,[29] and subsequent dissociation occurs at ground S_0 state surface:

$$S_0 + h\nu \rightarrow S_1 \qquad \text{(Formaldehyde photolysis)}$$
$$S_1 \rightarrow S_0^*$$
$$S_0^* \rightarrow H + HCO$$
$$S_0^* \rightarrow H_2 + CO$$

On the other hand, ISC almost completely dominates when propionaldehyde was irradiated with lower excitation energies,[29] and dissociation into radical products occurs at the lowest-lying triplet surface.

$$S_0 + h\nu \rightarrow S_1 \qquad \text{(Propionaldehyde photolysis)}$$
$$S_1 \rightarrow T_1$$
$$T_1 \rightarrow C_2H_5 + HCO$$

Acetaldehyde exhibits ~100% ISC at 330 nm, ~80% ISC at 315 nm, and essentially no ISC at 250 nm,[29] and radical products are formed from dissociation at both the vibrationally excited ground S_0 state surface and the first excited triplet state surface.

We have recently investigated the wavelength-dependent photolysis of *t*-pentanal ($(CH_3)_3CCHO$).[15] The Norrish II process is unavailable both from propionaldehyde and from *t*-pentanal photolysis, and the peak radical yield from the photodissociation of these two aldehydes is unity (see Figure 8). But the falloff of radical yields with decreasing wavelength is much faster in the *t*-pentanal case. For $\geq C_3$ aldehydes, the production of radical products has been correlated with the triplet state of aldehydes. Molecular products are formed from dissociation at highly vibrationally excited states in S_0 following IC and these products become increasingly important at shorter photolysis wavelengths. Therefore, the difference in the falloff behavior at shorter photodissociation wavelengths may reveal the difference in the excited-state singlet−triplet surface crossing of these two molecules. Theoretical interpretation of this difference might come from future publication by Francisco.[30]

Photodissociation Rate Constants to Form HCO Radicals in the Atmosphere. The rate constant (k_{rad}) for HCO production (or HO_2 in the presence of air) from the photolysis of propionaldehyde in the atmosphere was calculated from the following: the actinic solar flux ($J(\lambda)$) reported by Demerjian and co-workers;[31] the absorption cross section of propionaldehyde ($\sigma(\lambda)$); and the HCO radical yield at 760 Torr N_2 pressure ($\phi(\mathrm{HCO}, \lambda)$), using the relationship

$$k_{rad} = \Sigma\sigma(\lambda)\cdot\phi(\mathrm{HCO}, \lambda)\cdot J(\lambda)\Delta\lambda \qquad (15)$$

Since no quenching of the excited aldehyde precursor to dissociation by nitrogen was observed in the present study, the HCO radical yields from the photolysis of propionaldehyde at 760 Torr N_2 pressure were set equal to the HCO yields extrapolated to zero propionaldehyde pressure. Radical formation rate constants from propionaldehyde photolysis were calculated as a function of zenith angle under cloudless conditions at sea level and for best-estimate albedo; the results are shown in Figure 9. Our estimated radical formation rate constants were on the order of 4.6×10^{-5}, 3.8×10^{-5},and 1.6×10^{-5} s^{-1} for zenith angles of 0°, 30°, and 60°. Shepson and Heicklen[9] estimated radical formation rate constants from propionaldehyde photolysis to be 1.3×10^{-5} s^{-1} and 0.97×10^{-5} s^{-1} at zenith angles of 30° and 58.18°. Radical formation rate constants reported by Heicklen and co-workers[10] were 2.4×10^{-5} s^{-1} and 1.6×10^{-5} s^{-1} at zenith angles of 30° and 58.18°. Thus, our radical formation rate constants are a factor of 2.9 and 1.6 those reported by Shepson and Heicklen[9] and by Heicklen and co-workers[10] for a zenith angle of 30° and a factor of 1.6 and 1.0 for a zenith angle of 60°. Our calculation was made by assuming there was no quenching of the excited state of aldehyde by air. If there were an oxygen quenching effect, the radical formation rate constants in air would be smaller than those given here. Since the dominant photolysis pathway for propionaldehyde in the actinic UV region is formation of C_2H_5 + HCO, the total photolysis rate constant of propionaldehyde is approximately equal to its radical production rate constant. Atmospheric photodissociation lifetimes of propionaldehyde thus obtained were 6.0−17.4 h for zenith angles in the 0−60° range. Lifetime of propionaldehyde with respect to the OH radical reaction is on the order of 16.3 h for a globally averaged OH radical concentration of 10^6 molecules cm^{-3} and an OH/propionaldehyde reaction rate constant[1,3] of 1.7×10^{-11} cm^3 $molecule^{-1}$ s^{-1}. Therefore, both photolysis and the OH radical reaction are important removal pathways for propionaldehyde in the atmosphere.

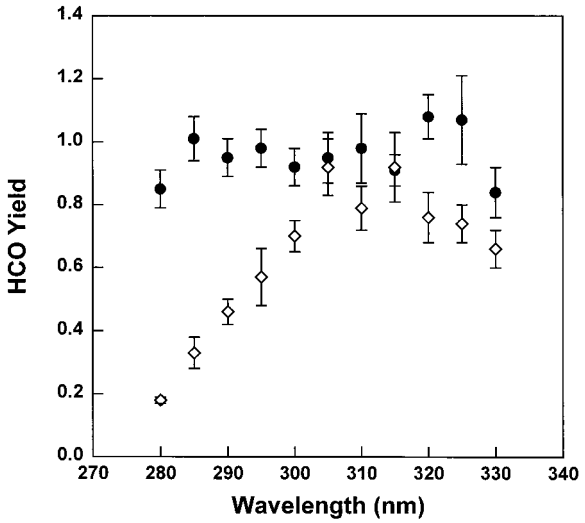

Figure 8. Wavelength dependency of HCO radical yields from propionaldehyde vs *t*-pentanal photolysis. Circles, propionaldehyde; diamonds, *t*-pentanal.

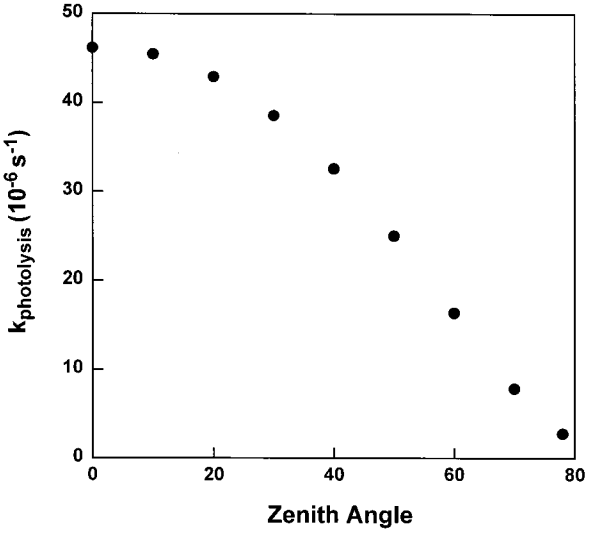

Figure 9. Atmospheric photodissociation rate constants of C_2H_5CHO to form radicals as a function of zenith angles at 760 Torr nitrogen pressure.

Conclusions

We have investigated photodecomposition of propionaldehyde in the 280−330 nm region by using dye laser photolysis in conjunction with cavity ring-down spectroscopy. Absorption cross sections of propionaldehyde were obtained. The HCO radical was a photodissociation product. The HCO radical yield and its dependence on photodissociation wavelength, propionaldehyde pressure, and nitrogen buffer gas pressure were determined. Wavelength dependency of radical yields from propionaldehyde photolysis was remarkably different from that obtained from *t*-pentanal photolysis at the shorter-wavelength tail, perhaps indicating a difference in the excited-states singlet−triplet surface crossing of these two molecules. Cross section results were combined with quantum yield information to calculate atmospheric photolysis rate constants of propionaldehyde to form HCO (or HO_2 in the presence of air) as a function of zenith angle for cloudless conditions at sea level and at 760 Torr nitrogen pressure. Atmospheric photodissociation lifetimes of propionaldehyde were on the order of 6.0−17.4 h for zenith angles in the 0−60° range.

Acknowledgment. We thank Professor Roger Atkinson for suggesting this project. Helpful discussion with Dr. Geoffrey Tyndall and constructive comments from an anonymous reviewer are acknowledged. We are grateful for the support provided by the National Science Foundation under grant Nos. ATM-9610285 and ATM-0000252.

References and Notes

(1) Semmes, D. H.; Ravishankara, A. R.; Gump-Perkins, C. A.; Wine, P. H. *Int. J. Chem. Kinet.* **1985**, *17*, 303.
(2) Dóbé, S.; Khachatryan, L. A.; Bérces, T. *Ber. Bunsen-Ges. Phys. Chem.* **1989**, *93*, 847.
(3) Kerr, J. A.; Sheppard, D. W. *Environ. Sci. Technol.* **1981**, *15*, 960.
(4) Tyndall, G. S.; Staffelbach, T. A.; Orlando, J. J.; Calvert, J. G. *Int. J. Chem. Kinet.* **1995**, *27*, 1009.
(5) Moortgat, G. K.; Seiler, W.; Warneck, P. *J. Chem. Phys.* **1983**, *78*, 1185.
(6) Carmely, Y.; Horowitz, A. *Int. J. Chem. Kinet.* **1984**, *16*, 1585.
(7) Ho, P.; Bamford, D. J.; Buss, R. J.; Lee, Y. T.; Moore, C. B. *J. Chem. Phys.* **1982**, *76*, 3630.
(8) Horowitz, A.; Calvert, J. G. *J. Phys. Chem.* **1982**, *86*, 3105.
(9) Shepson, P. B.; Heicklen, J. *J. Photochem.* **1982**, *19*, 215.
(10) Heicklen, J.; Desai, J.; Bahta, A.; Harper, C.; Simonaitis, R. *J. Photochem.* **1986**, *34*, 117.
(11) Blacet, F. E.; Pitts, J. N., Jr. *J. Am. Chem. Soc.* **1952**, *74*, 3382.
(12) Terentis, A. C.; Knepp, P. T.; Kable, S. H. *J. Phys. Chem.* **1995**, *99*, 12704.
(13) Terentis, A. C.; Knepp, P. T.; Kable, S. H. *Proc. SPIE-Int. Soc. Opt. Eng.* **1995**, *2548*, 328.
(14) Cronin, T. J.; Zhu, L. *J. Phys. Chem. A* **1998**, *102*, 10274.
(15) Zhu, L.; Cronin, T.; Narang, A. *J. Phys. Chem. A* **1999**, *103*, 7248.
(16) Martinez, R. D.; Buitrago, A. A.; Howell, N. W.; Hearn, C. H.; Joens, J. A. *Atmos. Environ.* **1992**, *26A*, 785.
(17) O'Keefe, A.; Deacon, D. A. G. *Rev. Sci. Instrum.* **1988**, *59*, 2544.
(18) O'Keefe, A.; Scherer, J. J.; Cooksy, A. L.; Sheeks, R.; Heath, J.; Saykally, R. J. *Chem. Phys. Lett.* **1990**, *172*, 214.
(19) Zhu, L.; Johnston, G. *J. Phys. Chem. A* **1995**, *99*, 15114.
(20) Zhu, L.; Kellis, D.; Ding, C.-F. *Chem. Phys. Lett.* **1996**, *257*, 487.
(21) Stoeckel, F.; Schuh, M. D.; Goldstein, N.; Atkinson, G. H. *Chem. Phys.* **1985**, *95*, 135.
(22) Braun, W.; Herron, J. T. *ACUCHEM/ACUPLOT Computer Program for Modeling Complex Reaction Systems*; National Bureau of Standards: Gaithersburg, MD 1986.
(23) Baulch, D. L.; Cobos, C. J.; Cox, R. A.; Esser, C.; Frank, P.; Just, Th.; Kerr, J. A.; Pilling, M. J.; Troe, J.; Walker, R. W.; Warnatz, J. *J. Phys. Chem. Ref. Data* **1992**, *21*, 411.
(24) Atkinson, R.; Baulch, D. L.; Cox, R. A.; Hampson, R. F., Jr.; Kerr, J. A.; Troe, J. *J. Phys. Chem. Ref. Data* **1992**, *21*, 1125.
(25) Baggott, J. E.; Frey, H. M.; Lightfoot, P. D.; Walsh, R. *J. Phys. Chem.* **1987**, *91*, 3386.
(26) Meller, R.; Moortgat, G. K. *J. Geophys. Res.* **2000**, *105*, 7089.
(27) Maric, D.; Burrows, J. P.; Meller, R.; Moortgat, G. K. *J. Photochem. Photobiol., A: Chem.* **1993**, *70*, 205.
(28) Ninomiya, Y.; Goto, M.; Hashimoto, S.; Kagawa, Y.; Yoshizawa, K.; Kawasaki, M.; Wallington, T. J.; Hurley, M. D. *J. Phys. Chem. A* **2000**, *104*, 7556.
(29) Lee, E. K. C.; Lewis, R. S. *Adv. Photochem.* **1980**, *12*, 1.
(30) Francisco, J. Private communication, 2001.
(31) Demerjian, K. L.; Schere, K. L.; Peterson, J. T. *Adv. Environ. Sci. Technol.* **1980**, *10*, 369.